

# Theory for the electron excitation in dielectrics under an intense circularly polarized laser field

Tomohito Otobe

*Kansai Photon Science Institute, National Institutes for Quantum and Radiological Science and Technology (QST), Kyoto 619-0215, Japan*

Yasushi Shinohara

*Photon Science Center, School of Engineering, The University of Tokyo, Hongo, Tokyo 113-8654, Japan*

Shunsuke A. Sato

*Graduate School of Pure and Applied Sciences, University of Tsukuba, Tsukuba 305-8571, Japan*

Kazuhiro Yabana

*Center for Computational Sciences, University of Tsukuba, Tsukuba 305-8571, Japan*

We report a Keldysh-like model for the electron transition rate in dielectrics under an intense circularly polarized laser. We assume a parabolic two-band system and the Houston function as the time-dependent wave function of the valence and conduction bands. Our formula reproduces the experimental result for the ratio of the excitation rate between linear and circular polarizations for  $\alpha$ -quartz. This formula can be easily introduced into simulations of nanofabrication using an intense circularly polarized laser.

## I. INTRODUCTION

Technical developments in femtosecond laser processing have made it possible to produce nanoscale laser-induced periodic surface structure (LIPSS), and realize, non-thermal ablation for sub-wavelength resolution [1–4].

Electron excitation in dielectrics by an intense laser field is the main process in laser-matter interactions. In particular, for femtosecond lasers, electron excitation by multiphoton ionization and tunnel ionization are the crucial, because such nonlinear processes generate a controllable free-carrier density and confine material change to the focal volume. Therefore, predicting the electron excitation rate using theoretical models and/or numerical simulation is important.

We have been developed a first-principles numerical method to explore electron excitation under an intense laser field using time-dependent density functional theory (TDDFT) [5–9]. This approach is currently the most reliable and accurate method with feasible computational cost to simulate electron excitation under intense laser fields. However, an analytical model may also be a helpful tool to understand some fundamental physical processes in laser processing.

Keldysh proposed a theory for the electron excitation rate under an intense linearly polarized laser field [10]. His approach is very general and can be used to describe the photoionization of different objects from single atoms to crystals [11]. Because of its generality, the Keldysh model has attracted much attention and become one of the standard tools in the theory of laser photoionization. In particular, for atoms and molecules, the Keldysh-Faisal-Reiss (KFR) theory [10, 12, 13], which is an implementation of the original Keldysh work, is one of the most important theories in understanding the

electron-laser interaction.

Recently, Temnov *et al* reported that the electron excitation rate induced by a circularly polarized laser is twice that induced by a linearly polarized laser at the same laser irradiance [15]. Circularly polarized lasers are also important as an ultrafast laser waveguides [16], and in controlling laser-induced nanostructures [17]. The purpose of this work is to construct an analytical formula for the transition probability in dielectrics including multiphoton and tunneling processes under a circularly polarized laser. We derive the transition probability in a crystalline solid under a circularly polarized laser assuming a parabolic two-band system and using the Houston function [18] as the time-dependent wave function.

Jones and Reiss [19] pioneered work on the electron excitation rate under a circular polarized laser employing the  $S$ -matrix theory. Although the Keldysh formula treats the time-dependent wave function of the valence and conduction bands as the Houston function and includes only the reduced mass, the Jones formula treats only the conduction band as the Houston function (Volkov state) and includes the effective mass of valence and conduction bands independently. Therefore, a direct comparison between the Keldysh and Jones formulas is not possible. In the case of atoms, Perelomov *et al.* [14] reported the analytical formula for the ionization rate under a circularly polarized laser. Because our new formula for circular polarization depends only on the reduced mass, it can be compared directly with the Keldysh formula. We also construct a new formula for a linear polarization using a parabolic two-band system. The relative ratio of the electron excitation rate between our two formulas shows reasonable agreement with the experimental results obtained by Temnov *et al* [15].

The present article is organized as follows. In section

II, we present our formalism to calculate the transition probability per unit time in a crystalline solid. In section III, we describe our results for  $\alpha$ -quartz with linearly and circularly polarized laser fields. A summary is presented in section IV.

## II. FORMALISM

### A. Houston function

The static Schrödinger equation for a spatially periodic system in atomic units is

$$\epsilon_{n,\vec{k}}^G u_{n,\vec{k}}^G(\vec{r}) = \left[ \frac{1}{2m} (\vec{p} + \vec{k})^2 + V(\vec{r}) \right] u_{n,\vec{k}}^G(\vec{r}), \quad (1)$$

where  $\vec{p}$  is the momentum operator,  $\vec{k}$  is the Bloch wave vector,  $V(\vec{r})$  is the spatially periodic potential, and  $\epsilon_{n,\vec{k}}^G$  and  $u_{n,\vec{k}}^G(\vec{r})$  are the energy and wave function, respectively, of the  $n$ -th band for the Bloch wave vector  $\vec{k}$ .  $u_{n,\vec{k}}^G(\vec{r})$  satisfies the periodic boundary condition,  $u_{n,\vec{k}}^G(\vec{r} + \vec{R}) = u_{n,\vec{k}}^G(\vec{r})$ . The time-dependent Schrödinger equation under a time-dependent vector potential is described as

$$i \frac{\partial u_{n,\vec{k}}^G(\vec{r}, t)}{\partial t} = \left[ \frac{1}{2m} (\vec{p} + \vec{k} + \frac{e}{c} \vec{A}(t))^2 + V(\vec{r}) \right] u_{n,\vec{k}}^G(\vec{r}, t). \quad (2)$$

Here  $\vec{A}(t)$  is the vector potential of the applied laser field. Now, we assume the Houston function,

$$w_{n,\vec{k}}(\vec{r}, t) = u_{n,\vec{k} + \frac{e}{c} \vec{A}(t)}^G(\vec{r}) \exp \left[ -i \int^t \epsilon_{n,\vec{k} + \frac{e}{c} \vec{A}(t')}^G dt' \right]. \quad (3)$$

The time evolution of the Houston function is described as,

$$\frac{\partial w_{n,\vec{k}}(\vec{r}, t)}{\partial t} = \frac{e}{c} \frac{d\vec{A}(t)}{dt} \frac{\partial u_{n,\vec{k}}^G}{\partial \vec{k}} \Big|_{\vec{k} + \frac{e}{c} \vec{A}(t)} e^{-i \int^t \epsilon_{n,\vec{k} + \frac{e}{c} \vec{A}(t')}^G dt'} + \epsilon_{n,\vec{k} + \frac{e}{c} \vec{A}(t)}^G u_{n,\vec{k} + \frac{e}{c} \vec{A}(t)}^G(\vec{r}). \quad (4)$$

We assume that the time-dependent wave function  $u_{n,\vec{k}}(\vec{r}, t)$  can be expanded by the Houston function,

$$u_{n,\vec{k}}(\vec{r}, t) = \sum_{n'} C_{nn'}^{\vec{k}}(t) w_{n,\vec{k}}(\vec{r}, t). \quad (5)$$

The time evolution of the coefficient  $C_{nn'}^{\vec{k}}(t)$  can be expressed by the simple form,

$$\frac{\partial C_{nn'}^{\vec{k}}(t)}{\partial t} = \frac{e}{mc} \frac{d\vec{A}(t)}{dt} \frac{\langle u_{n',\vec{k} + \frac{e}{c} \vec{A}(t)}^G | \vec{p} | u_{n,\vec{k} + \frac{e}{c} \vec{A}(t)}^G \rangle}{\epsilon_{n',\vec{k} + \frac{e}{c} \vec{A}(t)}^G - \epsilon_{n,\vec{k} + \frac{e}{c} \vec{A}(t)}^G} \times \exp \left[ -i \int^t dt' \left( \epsilon_{n',\vec{k} + \frac{e}{c} \vec{A}(t')}^G - \epsilon_{n,\vec{k} + \frac{e}{c} \vec{A}(t')}^G \right) \right] \quad (6)$$

The transition from  $w_{n,\vec{k}}(\vec{r}, t)$  to  $w_{n',\vec{k}}(\vec{r}, t)$  in an arbitrary time interval  $[-T, T]$  has the following form

$$\tilde{C}_{nn'}^{\vec{k}} = -\frac{ie}{mc} \int_{-T}^T dt \vec{P}_{n'n}^{\vec{k}} \cdot \vec{A}(t) \times \exp \left[ -i \int^t dt' \left( \epsilon_{n',\vec{k} + \frac{e}{c} \vec{A}(t')}^G - \epsilon_{n,\vec{k} + \frac{e}{c} \vec{A}(t')}^G \right) \right] \quad (7)$$

where  $\vec{P}_{n'n}^{\vec{k}}$  is the transition momentum matrix,

$$\vec{P}_{n'n}^{\vec{k}} = \langle u_{n',\vec{k}}^G(\vec{r}) | \vec{p} | u_{n,\vec{k}}^G(\vec{r}) \rangle. \quad (8)$$

### B. Parabolic two-band system

The Keldysh formula assumes the band structure is,

$$\epsilon_{c\vec{k}} - \epsilon_{v\vec{k}} = B_g \sqrt{1 + \frac{\vec{k}^2}{\mu B_g}}. \quad (9)$$

In contrast, we used a parabolic two-band system: i.e.

$$\epsilon_{c,\vec{k}}^G - \epsilon_{v,\vec{k}}^G = B_g + \frac{\vec{k}^2}{2\mu}, \quad (10)$$

where index  $c$  ( $v$ ) represents the conduction (valence) band,  $B_g$  is the band gap, and  $\mu$  is the reduced mass.

#### 1. Circular polarization

We assumed a circularly polarized laser field,

$$\vec{A}(t) = A_0 (\hat{x} \cos \omega t + \hat{y} \sin \omega t), \quad (11)$$

where  $\hat{x}$  and  $\hat{y}$  are the unit vectors along the  $x$ - and  $y$ -directions, respectively. We assumed that the propagation direction of the light was along the  $z$ -axis. The coefficient  $C_{nn'}^{\vec{k}}$  in Eq. (7) for the two-band system ( $C_{cv}^{\vec{k}}$ ) can be written as

$$C_{cv}^{\vec{k}} = -\frac{ieA_0}{2mc} \int_{-T}^T dt \left( M_{vc\vec{k}}^- e^{i\omega t} + M_{vc\vec{k}}^+ e^{-i\omega t} \right) \times \exp \left[ -i \int^t dt' \left( \epsilon_{c,\vec{k} + \frac{e}{c} \vec{A}(t')}^G - \epsilon_{v,\vec{k} + \frac{e}{c} \vec{A}(t')}^G \right) \right], \quad (12)$$

where

$$M_{vc\vec{k}}^{\pm} = P_{vc,x}^{\vec{k}} \pm iP_{vc,y}^{\vec{k}}. \quad (13)$$

The exponential part of Eq. (12) can be expanded by Bessel functions

$$\exp \left[ -i \int^t dt' \left( \epsilon_{c,\vec{k} + \frac{e}{c} \vec{A}(t')}^G - \epsilon_{v,\vec{k} + \frac{e}{c} \vec{A}(t')}^G \right) \right] = \exp \left[ -i \left( B_g + U_c + \frac{k^2}{2\mu} \right) t \right] \sum_l J_l(\eta) e^{il(\omega t - \phi)}, \quad (14)$$

where  $\phi$  is the angle between  $(k_x, k_y, 0)$  and the  $x$ -axis,  $\eta = ekA_0 \sin \theta / \mu\omega c$ , and  $U_c$  is the averaged kinetic energy of the charged particle in the circular polarized laser,  $U_c = e^2 A_0^2 / 2\mu c^2$ . The band gap is blue shifted by  $U_c$  [20], and  $\theta$  is the angle between the  $z$ -axis and  $\vec{k}$ .

The time-averaged transition probability per unit time and space,  $\tau_k$ , is found from

$$\tau_k = \lim_{T \rightarrow \infty} \frac{|\tilde{C}_{cv}^{\vec{k}}|^2}{2T} = \frac{e^2 \pi A_0^2 |P_{vc}|^2}{2m^2 c^2} \times \sum_l \left( J_{l-1}^2(\eta) + J_{l+1}^2(\eta) \right) \delta(\xi_k), \quad (15)$$

where  $\xi_k = (B_g + U_c + k^2/2\mu + l\omega)$ . In this step, we assume that  $\vec{P}_{vc}^{\vec{k}}$  do not depend on  $\vec{k}$ .

Gertsvelf *et al* have reported that orientation dependence on the electron excitation rate is few ten's % even for  $\alpha$ -quartz [21]. This fluctuation is minor effect for our purpose in this work, estimation in order and/or factor accuracy. In the case of the interaction between a circularly polarized laser and solid, one may consider that the angular momentum conservation defines the selection rule for a transition. While the angular momentum transfer also depends on lattice structure and dynamics [22], we only focus on the electronic response in this theory.

The total transition probability induced by the laser field,  $W$ , is found to be:

$$W = \frac{e^2 A_0^2 |P_{vc}|^2 \mu^{3/2}}{\sqrt{2\pi} m^2 c^2} \sum_{l=l_0}^{\infty} \int d\theta \sin \theta \times \left( J_{l-1}^2(\eta') + J_{l+1}^2(\eta') \right) \sqrt{\zeta_l}, \quad (16)$$

where,

$$\eta' = \frac{eA_0 \sqrt{2\zeta_l} \sin \theta}{\sqrt{\mu\omega c}}, \quad (17)$$

and

$$\zeta_l = l\omega - (B_g + U_c). \quad (18)$$

In Eq. (16), we changed the definition of  $l$  to  $-l$ . The lowest order of  $l = l_0$  is the positive minimum value for  $\zeta_{l_0} > 0$ . Here,  $\theta$  is the angle between the propagation direction of the laser ( $z$ -axis) and  $\vec{k}$ . The integration about the  $|\vec{k}|$  is replaced by the summation about  $l$  because of the  $\delta$ -function in Eq. (16).

In the low intensity limit, the dominant term in  $W$  is  $J_{l_0-1}$  which has a  $A_0^{2(l_0-1)}$  dependence. Because this coefficient includes  $A_0^2$ , the intensity dependence has the usual multiphoton absorption behavior of  $W \propto I^{l_0}$ .

## 2. Linear polarization

To compare linear and the circular polarizations, here we revisit the excitation rate under a linearly polarized

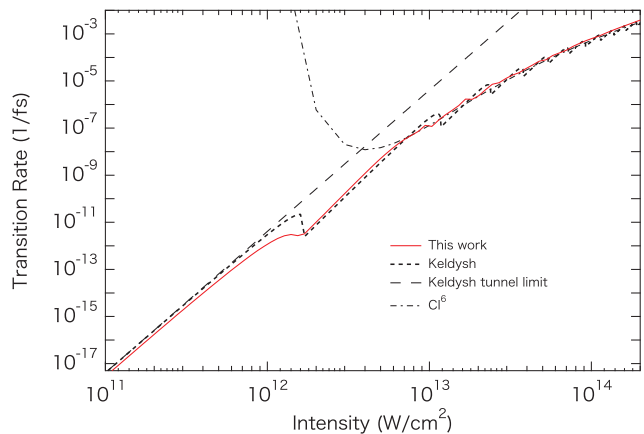


FIG. 1. Transition probability as a function of laser intensity for linearly polarized 800-nm light in  $\alpha$ -SiO<sub>2</sub>. The red solid line represents the excitation rate determined by our formalism, the blue dashed line represents the excitation rate based on the full expression of the Keldysh theory, the green dotted line represents the tunneling limit of the Keldysh theory, and the black dot-dashed line represents the simple six-photon process.

laser. We assumed a linearly polarized continuous wave field,

$$\vec{A}(t) = A_0 \hat{u} \cos \omega t, \quad (19)$$

$$\hat{u} = (0, 0, 1). \quad (20)$$

Following a similar procedure to that used for circular polarization, the total transition probability,  $W_L$ , is found from

$$W_L = \frac{e^2 A_0^2 |P_{vc}^{\vec{k}}|^2 \mu^{3/2}}{2\sqrt{2\pi} m^2 c^2} \int d\theta' \sin \theta' \times \sum_{l=l_0}^{\infty} (J_{l-1}(\alpha', \beta) + J_{l+1}(\alpha', \beta))^2 \sqrt{\kappa_l}, \quad (21)$$

where  $\kappa_l = l\omega - (B_g + U_p)$ ,  $\theta'$  is the angle between the polarization direction and  $\vec{k}$ , and  $l_0$  is the maximum integer  $l$  so that  $\kappa_l > 0$ .  $J_l(\alpha, \beta)$  is the generalized Bessel function [26] and  $U_p = e^2 A_0^2 / 4\mu c$  is the ponderomotive energy. Here,  $\alpha'$  and  $\beta$  are defined as

$$\alpha' = \frac{eA_0 \sqrt{2\kappa_l} \cos \theta'}{\sqrt{\mu\omega c}}, \quad (22)$$

and

$$\beta = \frac{e^2 A_0^2}{8\mu\omega c^2}. \quad (23)$$

## III. APPLICATION TO $\alpha$ -QUARTZ

### A. Linear polarization

$\alpha$ -Quartz is a typical dielectric used in non-linear laser-matter interaction studies, and we selected it here as an

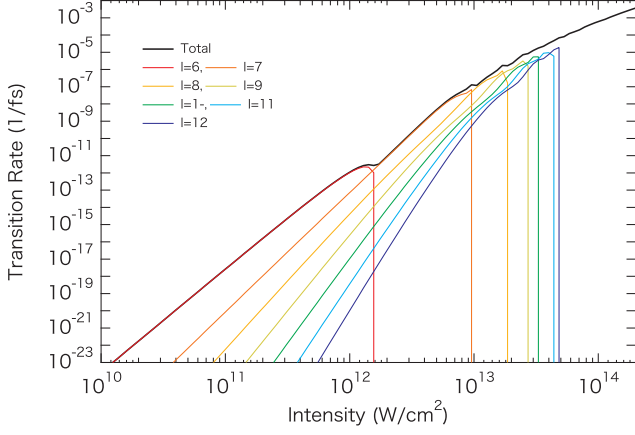


FIG. 2. Total transition probability for linear polarization as a function of laser intensity. The solid red curve is the same as that in Fig.1. The curves labeled  $l = 6, 7, \dots, 12$  give the separate contributions of each order.

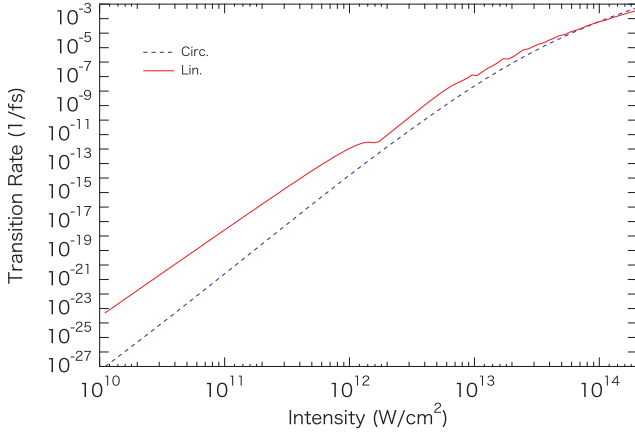


FIG. 3. Transition probability as a function of electric field intensity for linearly polarized (red solid line) and circularly polarized (blue dashed line) light.

example with which to illustrate the application of our developed formalism. The transition probability ( $W_L$ ) of  $\alpha$ -SiO<sub>2</sub> by linearly polarized 800nm light is shown in Fig. 1 by a red solid line. We assumed a band gap ( $B_g$ ) of 9 eV and reduced mass of  $0.30m$  [23]. For the momentum matrix element  $P_{cv}^{\vec{k}}$  we applied the Kane two-band model [24] giving,

$$|P_{cv}^{\vec{k}}|^2 \sim \frac{m^2 B_g}{4 \mu}. \quad (24)$$

In the case of  $\alpha$ -quartz, we assumed  $|P_{cv}|^2 \sim 0.28$  a. u. for  $B_g = 9$  eV and  $\mu = 0.30m$ .  $T$  calculated by the full expression of the conventional Keldysh formula (dashed line) and tunneling limit (dot-dashed line) are also shown in Fig. 1 for comparison. Our formalism shows excellent agreement with the Keldysh theory. This result indicates

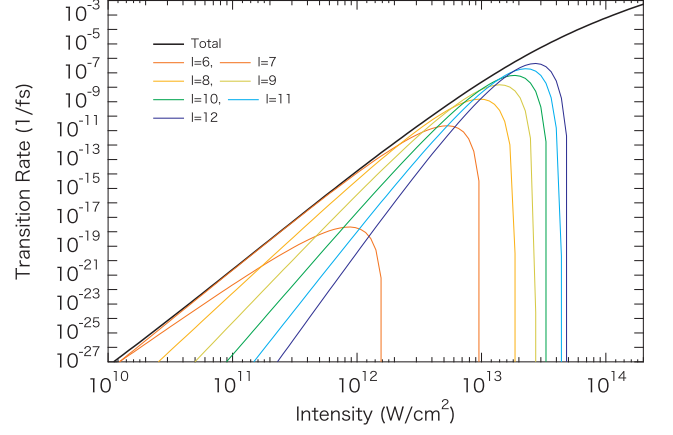


FIG. 4. Total transition probability for circular polarization as a function of electric field intensity. The solid red curve is the same as the blue dashed curve in Fig.3. The curve labels  $l = 6, 7, \dots, 12$  give the separate contribution of each order.

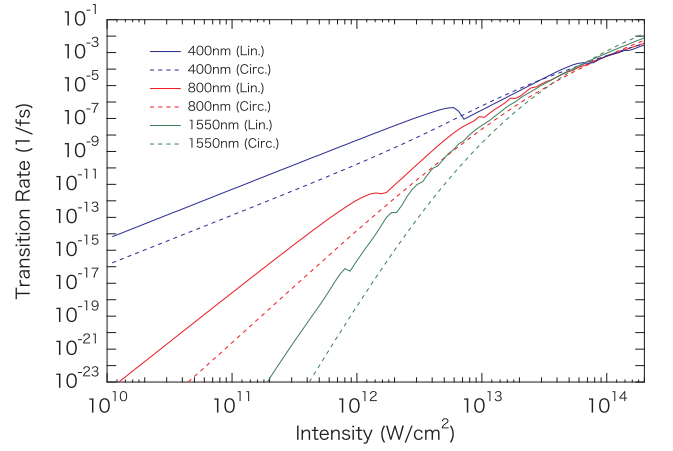


FIG. 5. Wavelength dependence of the total transition probability for circular and linear polarizations as a function of laser intensity. Solid curves represent linear polarization, and dashed lines represent circular polarization.

that our formula includes the multiphoton and tunneling processes as the Keldysh formula does.

At lower intensity, the transition probability is expected to depend on the laser intensity  $I$  as  $W_L \propto CI^l$ , with  $l = 6$  in the multiphoton absorption picture. We show a curve of this dependence in Fig. 1 with the green dotted line. Our result maintains this picture up to  $5 \times 10^{11}$  W/cm<sup>2</sup>.

Because the ponderomotive energy  $U_p$  widens the band gap as the laser intensity increases, the contribution of each  $l$ -photon process also changes. Figure 2 presents the contribution of each  $l$ -photon process to  $T$  as a function of the maximum electric field intensity. At around  $1 \times 10^{11}$  W/cm<sup>2</sup>, the probability of the six-photon absorption falls to zero, because the effective band gap ( $B_g + U_p$ ) is larger than  $6\hbar\omega$  at this point, and the seven-photon

process becomes dominant. Simultaneously, the change of the order of the multiphoton process induces a small jump in  $T$  which is also seen in the Keldysh formula and its extended model developed by Gruzdev[25]. This abrupt change of the  $l$ -photon process indicates that the averaged kinetic energy  $U_p$  defines the effective band gap which is similar to the blue shift of the band gap in the dynamical Franz-Keldysh effect [20, 27]. However, the critical intensity for higher multi-photon processes is slightly different from that determined by the Keldysh formula which may originate from the definition of the band structure.

In a higher intensity region, over  $1 \times 10^{13}$  W/cm<sup>2</sup>, the contributions from some  $l$ -photon processes are comparable. In this intensity region, the tunneling model is valid because the Keldysh parameter,  $\gamma = c\sqrt{\mu B_g}/eA_0$ , is less than one. Therefore, this result shows that the tunneling process can be interpreted as the summation of many multi-photon processes.

### B. Circular polarization

The transition rate induced by circularly polarized 800-nm light as a function of laser intensity is illustrated in Fig.3 as a blue dashed line. The transition rate induced by linearly polarized 800-nm light is also shown as a solid red line. The power law of the transition rate induced by the circularly polarized light is slightly different from that for linearly polarized light and higher than that for linearly polarized light of higher intensity. Temnov *et al* [15] reported the ratio of the ionization rate around an intensity of  $1 \times 10^{13}$  W/cm<sup>2</sup>. From the relation between the intensity in vacuum ( $I_v$ ) and in media ( $I_m$ ),  $I_m = \varepsilon^{1/2}I_v$  where  $\varepsilon$  is the dielectric constant,  $1 \times 10^{13}$  W/cm<sup>2</sup> corresponds to  $4 \times 10^{12}$  W/cm<sup>2</sup> in Fig. 3. The experimental value for the excitation rate ratio  $W/W^l$  is 0.3. Our result gives a ratio of  $0.1 \sim 0.2$  at  $2 \times 10^{12} \sim 1 \times 10^{13}$  W/cm<sup>2</sup> which is in reasonable agreement with the experimental value.

Figure 4 shows the contribution of each  $l$ -photon process to  $W$  as a function of the maximum electric field intensity. The change of the multiphoton process is not abrupt like in the case with linear polarization (Fig. 2) and the contribution of each photon processes is more important at lower intensity. In the circular polarization, the drop off of each  $l$ -photon process is more moderate compared with that induced by linearly polarized laser. This qualitative difference originates from the pa-

rameter dependence of the generalized and normal Bessel functions.

The contribution of each photon process is also different, because the kinetic energy of a charged particle under circularly polarized laser changes from  $U_p$  to  $U_c$ , which effectively shifts the optical band gap. Because  $U_c$  is larger than  $U_p$  by a factor of 2, which corresponds to a factor of  $\sqrt{2}$  in the field intensity,  $B_g + U_c$  exceeds  $6\hbar\omega$  at lower field intensity when polarization is circular rather than linear.

Laser wavelengths other than of 800 nm are also used for laser processing. For example, 400 nm (3.1 eV), which is the second harmonic of 800-nm, is useful to lower the order of multiphoton processes, and 1550 nm (0.8 eV) is the typical wavelength of fiber lasers. Figure 5 depicts the wavelength dependence of the total transition rates under linear (solid) and circular (dashed) polarizations.

For all wavelengths, above  $5 \times 10^{13}$  W/cm<sup>2</sup>, the transition rate induced by circular polarization is comparable to that induced by linear polarization. In contrast, at lower intensity, the ratio between circular and linear polarizations becomes large as the wavelength increases: i.e., as photon energy decreases.

## IV. SUMMARY

We extended the Keldysh-type formula for the solid state under an intense circularly polarized laser assuming the Houston function for the valence and conduction bands. Because our formula depends only on the reduced mass, it can be directly compared with the Keldysh formula. Our simple formula describes electron excitation rate, reproduces the Keldysh formula with excellent agreement for  $\alpha$ -quartz, and makes it possible to separate the contribution of each  $l$ -photon process with linear or circular polarization. The transition rate ratio between linear and circular polarizations determined using our formula shows reasonable agreement with experimental results.

## ACKNOWLEDGEMENT

This work was supported by a JSPS KAKENHI (Grants No. 21740303 and No. 15H03674). Numerical calculations were performed on the supercomputer PRIMERGY BX900 at the Japan Atomic Energy Agency (JAEA).

- 
- [1] K. M. Davis, K. Miura, N. Sugimoto, and K. Hirao, *Opt. Lett.* **21**, 1729 (1996) Writing waveguides in glass with a femtosecond laser.  
 [2] R. R. Gattass and E. Mazur, *Nat. Photonics* **2**, 219 (2008) Femtosecond laser micromachining in transparent

materials.

- [3] K. Miura, J.R. Qiu, H. Inouye, T. Mitsuyu, and K. Hirao, *Appl. Phys. Lett.* **71**, 3329 (1997) Photowritten optical waveguides in various glasses with ultrashort pulse laser.

- [4] V. R. Bhardwaj, et al, Phys. Rev. Lett. **96**, 057404 (2006) Optically Produced Arrays of Planar Nanostructures inside Fused Silica.
- [5] E. Runge and E. K. U. Gross, Phys. Rev. Lett. **52**, 997 (1984) Density-Functional Theory for Time-Dependent Systems.
- [6] G.F. Bertsch, J.-I. Iwata, A. Rubio, and K. Yabana, Phys. Rev. B **62**, 7998 (2000) Real-space, real-time method for the dielectric function.
- [7] T. Otobe, M. Yamagiwa, J. -I. Iwata, K. Yabana, T. Nakatsukasa, and G. F. Bertsch, Phys. Rev. B **77**, 165104 (2008) First-principles electron dynamics simulation for optical breakdown of dielectrics under an intense laser field.
- [8] Y. Shinohara, K. Yabana, Y. Kawashita, J.-I. Iwata, T. Otobe, and George F. Bertsch, Phys. Rev. B **82**, 155110 (2010) Coherent phonon generation in time-dependent density functional theory.
- [9] K. Yabana, T. Sugiyama, Y. Shinohara, T. Otobe, and G. F. Bertsch, Phys. Rev. B **85**, 045134 (2012) Time-dependent density functional theory for strong electromagnetic fields in crystalline solids.
- [10] L. V. Keldysh, Sov. Phys. JETP **20**, 1307 (1965) Ionization in the Field of a Strong Electromagnetic Wave.
- [11] S.M. Golin, S. E. Kirwood, D. D. Klug, D. M. Villeneuve, D. M. Rayner, C. A. Trallero Herrero, and P. B. Corkum, J Phys. B: At. Mol. Opt. Phys. **47**, 204025 (2014) Strong field processes inside gallium arsenide.
- [12] F. H. M. Faisal, J. Phys. B: At. Mol. Opt. Phys. **6**, L89 (1973) Multiple absorption of laser photons by atoms.
- [13] H. R. Reiss, Phys. Rev. A **22**, 1786 (1980) Effect of an intense electromagnetic field on a weakly bound system.
- [14] A. M. Perelomov, S. V. Popov and V. M. Terentev, Sov. Phys. JETP **23**, 924 (1966) Ionization of atoms in an alternating electric field
- [15] V.V. Temnov, K. Sokolowski-Tinten, P. Zhou, A. El-Khamhawy, and D. von der Linde, Phys. Rev. Lett. **97**, 237403 (2006) Multiphoton Ionization in Dielectrics: Comparison of Circular and Linear Polarization.
- [16] Amir H. Nejadmalayeri and Peter R. Herman, Optics Letters **31**, 2987 (2006) Ultrafast laser waveguide writing: lithium niobate and the role of circular polarization and picosecond pulse width.
- [17] Min Huang, Fuli Zhao, Ya Cheng, Ningsheng Xu, and Zhizhan Xu, Optics Express **16**, 19354 (2008) Large area uniform nanostructures fabricated by direct femtosecond laser ablation.
- [18] W. V. Houston, Phys. Rev. **57**, 184 (1940) Acceleration of Electrons in a Crystal Lattice.
- [19] H. D. Jones and H. R. Reiss, Phys. Rev. B **16**, 2466 (1977) Intense-field effects in solids.
- [20] A. P. Jauho and K. Johnsen, Phys. Rev. Lett. **76**, 4576 (1996) Dynamical Franz-Keldysh Effect.
- [21] M. Gertsvelf, H. Jean-Ruel, P. P. Rajeev, D. D. Klug, D. M. Rayner, and P. B. Corkum, Phys. Rev. Lett. **101**, 243001 (2008) Orientation-Dependent Multiphoton Ionization in Wide Band Gap Crystals.
- [22] H. J. Simon and N. Bloembergen, Phys. Rev. **171**, 1104 (1968) Second-Harmonic Light Generation in Crystals with Natural Optical Activity.
- [23] B. Brar, G. D. Wilk, and A. C. Seabaugh, Appl. Phys. Lett. **69**, 2728 (1996) Direct extraction of electron tunneling effective mass in ultrathin SiO<sub>2</sub>.
- [24] E. O. Kane, J. Phys. Chem. Solids **12** 181 (1959) Zener tunneling in semiconductors.
- [25] V. E. Gruzdev, Phys. Rev. B **75**, 205106 (2007) Photoionization rate in wide band-gap crystals.
- [26] H. R. Reiss and V. P. Krainov, J. Phys. A: Math. Gen. **36**, 5575 (2013) Generalized Bessel functions in tunnelling ionization.
- [27] K. B. Nordstrom, K. Johnsen, S. J. Allen, A.-P. Jauho, B. Birnir, J. Kono, T. Noda, H. Akiyama, and H. Sakaki, Phys. Rev. Lett. **81**, 457 (1998) Excitonic Dynamical Franz-Keldysh Effect.